

## Coupled disease-vaccination behavior dynamic analysis and its application in COVID-19 pandemic



Xueyu Meng<sup>a,b,c</sup>, Jianhong Lin<sup>c,d</sup>, Yufei Fan<sup>a,b</sup>, Fujuan Gao<sup>c</sup>, Enrico Maria Fenoaltea<sup>c</sup>, Zhiqiang Cai<sup>a,b,\*</sup>, Shubin Si<sup>a,b,\*</sup>

<sup>a</sup> Department of Industrial Engineering, School of Mechanical Engineering, Northwestern Polytechnical University, Xi'an 710072, China

<sup>b</sup> Ministry of Industry and Information Technology Key Laboratory of Industrial Engineering and Intelligent Manufacturing, Northwestern Polytechnical University, Xi'an 710072, China

<sup>c</sup> Department of Physics, University of Fribourg, Fribourg 1700, Switzerland

<sup>d</sup> Department of Management, Technology and Economics, ETH Zürich, Scheuchzerstrasse 7, CH-8092 Zürich, Switzerland

### ARTICLE INFO

#### Keywords:

Epidemic spreading  
Vaccination behavior  
Compartment model  
Evolutionary game theory  
COVID-19

### ABSTRACT

Predicting the evolutionary dynamics of the COVID-19 pandemic is a complex challenge. The complexity increases when the vaccination process dynamic is also considered. In addition, when applying a voluntary vaccination policy, the simultaneous behavioral evolution of individuals who decide whether and when to vaccinate must be included. In this paper, a coupled disease-vaccination behavior dynamic model is introduced to study the coevolution of individual vaccination strategies and infection spreading. We study disease transmission by a mean-field compartment model and introduce a non-linear infection rate that takes into account the simultaneity of interactions. Besides, the evolutionary game theory is used to investigate the contemporary evolution of vaccination strategies. Our findings suggest that sharing information with the entire population about the negative and positive consequences of infection and vaccination is beneficial as it boosts behaviors that can reduce the final epidemic size. Finally, we validate our transmission mechanism on real data from the COVID-19 pandemic in France.

### 1. Introduction

Over the years, prevention and control of the spread of infectious diseases have been key research topics for scientists. Currently, quarantine and vaccination are two effective ways to control the spread of infectious diseases in the short and long term, respectively [1–4]. Regarding vaccination measures, previous studies have mainly focused on mandatory vaccination. In this paper, our goal is to analyze the dynamics of vaccination behavior when vaccination is voluntary and its impact on the disease spreading.

Traditional models for the spread of infectious diseases are the so-called compartment models, including the SIS (susceptible-infected-susceptible) and the SIR (susceptible-infected-recovered) models [5–8], or the more sophisticated SIRS (susceptible-infected-recovered-susceptible) and SEIR (susceptible-exposed-infected-recovered) models [9–12], among many others. In these models, individuals in the population are divided into different compartments that describe their status (susceptible or infected, for example). One can derive the differential

equations describing the dynamics of these systems. Analyzing the equilibrium point of these differential equations, one can find the final epidemic size (FES), i.e., the total number of people experiencing infection during the outbreak [13]. In general, the equilibrium points of such dynamic systems include the disease-free equilibrium point (DFE) and the endemic equilibrium point (EE) [14,15]. In addition, a key parameter is the basic reproduction number, i.e., an index that describes the infection rate and gives information on the epidemic's potential [3,16].

Although the traditional spreading models describe the spreading behavior of many diseases, they have important limitations, as they ignore the heterogeneity of the infectious capacity of different individuals in different places and times [12,17,18]. To overcome these limitations, the impact of disease spreading (and its prevention) has also been studied on different social network structures. Here, the interactions between individuals are modeled as the links in a social network whose nodes are the individuals themselves [19,20]. Whether diseases, computer viruses or rumors, their spread is inevitably

\* Corresponding authors at: Department of Industrial Engineering, Northwestern Polytechnical University, Xi'an 710072, China.

E-mail addresses: [caizhiqiang@nwpu.edu.cn](mailto:caizhiqiang@nwpu.edu.cn) (Z. Cai), [sisb@nwpu.edu.cn](mailto:sisb@nwpu.edu.cn) (S. Si).

influenced by the topology and structure of the social network [21–23]. In 1998, Watts and Strogatz proposed the small world network [24]. In 1999, Barabasi and Albert proposed the preferential attachment mechanism for generating scale-free networks [25]. Since then, the theory of complex networks has developed rapidly. The proposal and derivation of many network models provide a new direction for the study of infectious diseases, of which three are the most pioneering. The first is the mean-field model proposed by Pastor-Satorras and Vespignani in 2001 [26,27]. The second is the infiltration model proposed by Newman in 2002 [28]. The third is the discrete probability model proposed by Wang in 2003 [29]. Models of disease spreading on more advanced networks, such as multilayer networks and adaptive networks, have also been investigated [30,31]. For example, Zhu et al. proposed a two-layer network model to study the spreading properties of lethal diseases [32]. Gao et al. introduced a model on multiplex networks with the presence of self-diffusion and cross-diffusion [33].

On the other hand, to study the populations behavior with respect to vaccination, evolutionary game theory has been implemented [34,35]. When a policy of voluntary vaccination is adopted, the individual decision to vaccinate depends on multiple factors, such as individual infection risk, vaccination cost, vaccine safety, etc. [36,37]. Using game theory, one can quantify individuals' decision-making based on these factors [38,39] (note that also evolving vaccination games depend on the structure of the social networks). When individuals in the population are continuously vaccinated, the spread of disease is limited and the risk of infection of unvaccinated people is reduced. As a result, some unvaccinated individuals, called "free riders", are indirectly protected [40–42]. However, infectious diseases spread more effectively among the unvaccinated population. These two contrasting effects generate the so-called "vaccination dilemma" [43–46]. Evolutionary game theory can well describe the decision-making behavior when individuals are faced with this dilemma [47–49].

In general, when an individual's perceived risk of infection increases, she will choose a specific vaccination strategy (i.e., to vaccinate or not) with a probability that depends on a risk-benefit analysis [50–53]. Hence, individuals constantly update their strategies to maximize their interests. The individual strategy learning process includes two aspects: one is the mechanism of self-learning, such as learning by reinforcement [54]; the other is the imitation mechanism, based, for example, on Fermi's updating rules [55–58] (as we shall explain in more detail below). According to some scholars, without the intervention of incentive measures, the population cannot inhibit the spread of diseases with a voluntary vaccination policy [38,59]. Within the framework of evolutionary game theory, however, it has been found that imitating the vaccination strategy of hub nodes can effectively inhibit the transmission of infectious diseases [41,42,60]. Today, understanding how control measures and people's behavior affect the spread of the disease is an urgent issue given the rapid spread of COVID-19 [61,62].

The literature that investigates the interplay between disease dynamics and vaccination behavior is constantly growing [34,63,64]. So far, the evolution of epidemic and vaccination behavior are treated as two distinct processes: at a given time, individuals decide whether to vaccinate based on the epidemiological outcomes of the previous period; at this point, the vaccination rate is observed and then the scale of infection transmission of subsequent times is analyzed, until the next temporal instant when individuals update again their strategies. This approach is suitable for modeling seasonal viruses such as influenza in which people, before the season of the diffusion peak, adjust their vaccination behavior based on the results of the previous season. However, the pandemic experience of the past two years and the properties of the COVID-19 virus suggest that we are facing a scenario in which disease dynamics and vaccination behaviors co-evolve in a single process.

In light of this, our goal in this paper is to investigate the transmission of infectious diseases and the simultaneous vaccination process from an evolutionary point of view. As mentioned above, individuals

decide their vaccination strategy by performing a cost-benefit analysis that can be different in different stages of the epidemic. Thus, also vaccination strategies evolve together with the disease transmission process. In the following, these mechanisms are integrated into a new dynamic coupled behavior model of vaccination to study the coevolution of vaccination strategies and disease spreading as a unique process. Note, however, that vaccination is not the only defense against contagion and infection: there are other protective measures such as wearing masks and hand washing, among many others. For simplicity, we only address vaccination in this paper, but the effects of other protective measures on our modeling approach can be studied in the future.

Our main contribution is threefold. First, we introduce a new coupled disease- vaccination behavior dynamic which extends and complements the work of Kabir and Tanimoto in [34]. In our model, the population is abstracted as a social network where nodes are individuals and edges represent their interactions. The mechanism of disease transmission is studied by a compartmental model based on the mean-field theory. Here, we introduce an infection rate of susceptible individuals that is non-linear in the number of infected neighbors. Unlike the standard (linear and nonlinear) infection rates studied in the above-cited literature, which assume that at each time step an individual's infection probability depends on a single interaction, our infection rate takes into account the possible individual's simultaneous interaction with her neighbors. This describes a more realistic scenario where people have multiple contacts in the same time window.

Instead, the evolution of individual vaccination strategies is based on the evolutionary game theory. As in [34], we study two strategy updating rules: A local rule that considers only the individual benefit, and a global rule that considers the benefit of the whole population. In addition, since in the real world there is a lag time between the spread of the virus and the adoption of a given vaccine strategy, we analyze numerically how the observables in our model vary by varying this lag time.

Second, we analyze the main parameters of the model. The next-generation matrix method is used to obtain the basic reproduction number and identify the parameters' critical values for the evolution of vaccination and non-vaccination strategies.

Finally, we analyze real transmission data of COVID-19 in France to validate our infection transmission model. Our results suggest an early warning method for infectious disease outbreaks and can guide policymakers in their decisions.

The rest of this paper is organized as follows. Section 2 describes the new dynamic model of coupled disease-vaccination behavior. The reproduction number is studied in Section 3. Numerical simulations are shown in Section 4. Here, the dependence of disease spreading on model parameters is analyzed in detail with the phase diagrams of the evolution. In Section 5, we show the empirical analysis of COVID-19 data in France. Section 6 concludes the paper and discuss potential future researches and perspectives.

## 2. Coupled disease-vaccination behavior dynamic model

In this section, the new coupled disease-vaccination behavior dynamic model is introduced. We first describe the disease transmission process based on the mean-field approximation (MFA). Then, we show how the evolutionary game theory (EG) under two different updating rules is implemented for the vaccination strategies evolution.

### 2.1. Dynamic model of disease transmission based on mean-field theory

The population is divided into compartments according to the individuals' strategies and epidemic states. And there are two strategies, C and D, that represent the proportion of susceptible individuals adopting the vaccination strategy (cooperation strategy) and the susceptible proportion of individuals adopting the non-vaccination strategy (deception strategy), respectively. Furthermore, it is assumed that there

exist six epidemic states  $\{V_E, S_V, I_V, S_N, I_N, R\}$  with the following meanings:  $V_E$  is the proportion of individuals effectively vaccinated;  $S_V$  is the proportion of individuals ineffectively vaccinated (because of, for example, vaccine imperfection), and thus still susceptible;  $I_V$  is the proportion of individuals ineffectively vaccinated who has been infected;  $S_N$  is the proportion of non-vaccinated susceptible individuals;  $I_N$  is the proportion of individuals non-vaccinated and infected;  $R$  is the proportion of recovered individuals (after the infection). It is assumed that individuals in the state  $R$  have permanent immunity. A graphical representation of the interaction between compartments in our coupled disease-vaccination behavior dynamic model is shown in Fig. 1.

In the figure,  $e$  is the vaccination efficacy, meaning that the vaccine protects against infection with probability  $e$ , but is ineffective with probability  $1-e$ . This stochastic approach to modeling vaccine imperfection is called the effectiveness model [65]. This is complementary to the efficiency model, which, however, describes other protective measures, such as wearing a face mask, that are not considered in this paper [65]. Then  $\lambda$  is the probability that a susceptible individual is infected by her infected neighbors, i.e. it is the infection rate. Considering a homogeneous social network, we assume that an individual interacts at each time-step with all her neighbors. In this way,  $\lambda$  is equal to  $1-(1-\beta)^{\langle k \rangle(I_V+I_N)}$ , where  $\beta$  is the probability of disease transmission after contact with an infected person, and  $\langle k \rangle$  is the average degree of the network, i.e., the average number of neighbors of each individual. Of course, this infection rate is nonlinear with the number of neighbors. Moreover,  $\mu$  is the probability of an individual changing from an infected state to the  $R$  state. Table 1 provides a list of all parameters in our model with their corresponding meanings.

According to the described dynamic compartmental model, the system is described by the following differential equations:

**Table 1**  
Parameters of the coupled disease-vaccination behavior model.

Parameters	Description
$\beta$	The per-contact transmission probability
$\mu$	The probability from infected state to recovered state
$\lambda$	The probability that a susceptible individual will be infected by the infected neighbors
$\kappa$	The degree of rationality of an individual
$e$	The vaccination efficacy
$\langle k \rangle$	The average number of contacts in the population
$c$	The relative cost

$$\begin{cases} \frac{dS_V}{dt} = -S_V \left[ 1 - (1 - \beta)^{\langle k \rangle(I_V + I_N)} \right] + (1 - e)\Delta_1 - \Delta_2 \\ \frac{dS_N}{dt} = -S_N \left[ 1 - (1 - \beta)^{\langle k \rangle(I_V + I_N)} \right] - \Delta_1 + \Delta_2 \\ \frac{dI_V}{dt} = S_V \left[ 1 - (1 - \beta)^{\langle k \rangle(I_V + I_N)} \right] - \mu I_V \\ \frac{dI_N}{dt} = S_N \left[ 1 - (1 - \beta)^{\langle k \rangle(I_V + I_N)} \right] - \mu I_N \\ \frac{dV_E}{dt} = e\Delta_1 \\ \frac{dR}{dt} = \mu(I_V + I_N) \end{cases} \quad (1)$$

Here, the interaction terms  $\Delta_1$  is the proportion of the  $S_N$  individuals who switch from strategy D (non-vaccination) to strategy C (vaccination); on the contrary, the interaction term  $\Delta_2$  is the proportion of the  $S_V$  individuals who switch from strategy C to strategy D. The values of  $\Delta_1$  and  $\Delta_2$  are determined by the behavioral dynamic, as explained in details in Section 2.2.1. The solution set of the dynamic system (1) is

$$D = \{(S_V, S_N, I_V, I_N, V_E, R) \in R_+^6 : S_V(t) + S_N(t) + I_V(t) + I_N(t) + V_E(t) + R(t) = 1\}.$$

## 2.2. Imitation dynamic model of vaccination behavior based on the evolutionary game theory

The vaccination strategy evolution is described based on the EG in this section. As rules for updating the strategy, two risk assessment

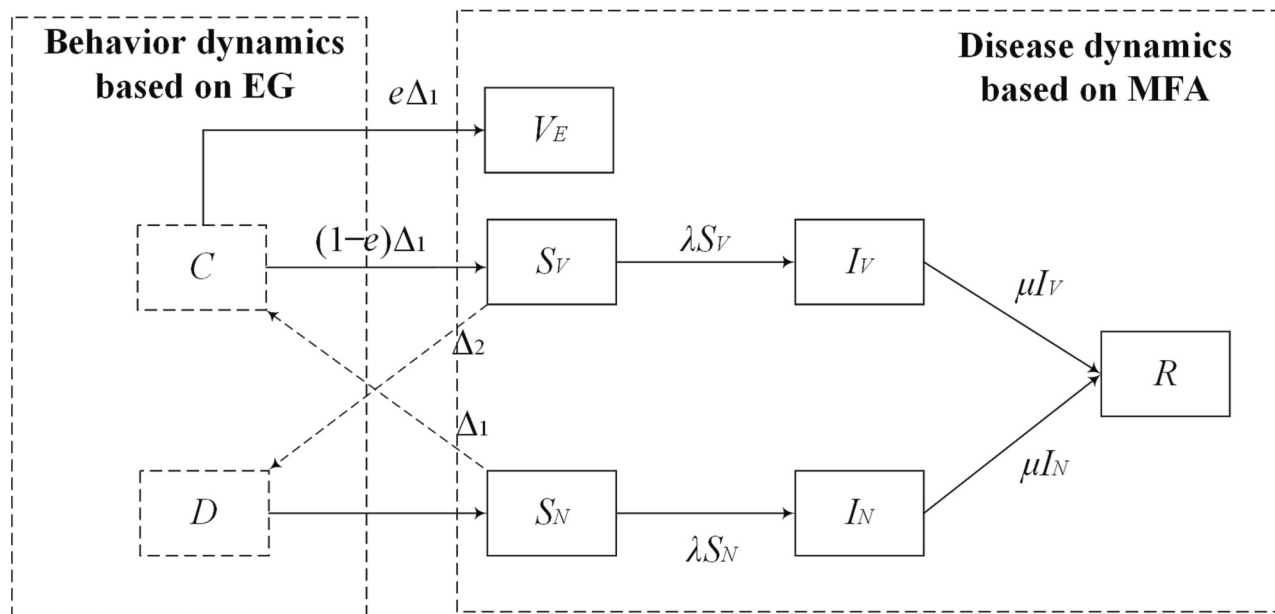


**Fig. 1.** Schematic representation of our coupled disease-vaccination behavior dynamic model.

methods are considered to characterize individual behavior in the imitation dynamics: an individual-based method and a society-based method. In the first case, the strategy update rule is described as follows. Each individual evaluates both the risk of maintaining her own strategy and that of imitating her neighbor's strategy. Then she selects the one with the lowest individual risk and the highest individual payoff. However, if the information about the consequences of adopting a certain strategy is public, individuals would no longer rely on the payoff of a single neighbor to evaluate risks. Instead, they would assess risk based on the average payoff of the society resulting from the choice of a certain strategy. To study this scenario, a society-based risk assessment rule is introduced to our model. Henceforth, we use the same terminology as in [34] and abbreviate the individual-based risk assessment as IB-RA and the society-based risk assessment as SB-RA.

### 2.2.1. Individual-based risk assessment (IB-RA)

Depending on the strategy choice, a susceptible individual (either in the  $S_V$  or in the  $S_N$  compartment) must consider five possible outcomes, as shown in the payoff matrix in Table 2.

Specifically, if the individual chooses to vaccinate (V), the vaccine may be effective ( $S_e$ ) or ineffective ( $S_{ie}$ ). In the former case, the cost corresponds only to the cost of vaccination  $C_V$  (in terms of money, time, or side effects) and we refer to this outcome as vaccination-effective-strategy (VES). In the second case, in addition to the cost of vaccination, one must add the cost of potential infection. This must be interpreted, for example, as a psychological cost due to the fear of becoming infected or the knowledge to be more vulnerable than effectively vaccinated people. It is also an economic cost caused by the social restrictions imposed by governments (e.g., prohibition to accessing certain public places) on susceptible individuals. For these reasons, we assume that a susceptible individual, even if not actually infected, incurs a cost proportional to the probability of becoming infected  $\lambda$  (the greater the probability of becoming infected, the greater the fear and the greater the social restrictions) and the cost to be paid in the event of infection (the greater that cost the greater the fear of becoming infected, for example). Hence, in the  $S_{ie}$  case, the payoff is  $-C_V - \lambda C_I$ , where the second addend is the cost of potential infection and  $C_I$  is the effective cost of infection (in terms of economic costs in treating the disease or psychological costs due, for example, to isolation). We refer to this outcome as the vaccination-non-effective-strategy (VNS). If the ineffectively vaccinated individual actually becomes infected, the cost to be incurred would be the cost of vaccination plus the effective cost of infection. In this case, we refer to this outcome as the vaccination-infection strategy (VNI). Instead, if the individual decides not to vaccinate (N), the cost corresponds only to the cost of potential infection defined above, and we refer to this outcome as the non-vaccination-susceptible strategy (NS). If the non-vaccinated individual actually becomes infected, the cost to be incurred would be the effective cost of infection and we refer to this outcome as the non-vaccination-infection strategy (NI).

Denoting as  $\pi_i$  the payoff of outcome  $i$ , we can write

$$\begin{cases} \pi_{VES} = -C_V \\ \pi_{VNS} = -C_V - \lambda C_I \\ \pi_{VNI} = -C_V - C_I \\ \pi_{NS} = -\lambda C_I \\ \pi_{NI} = -C_I \end{cases} \quad (2)$$

**Table 2**  
The payoff matrix.

	Health		Infected
V	$S_e$ $-C_V$ [VES]	$S_{ie}$ $-C_V - \lambda C_I$ [VNS]	$-C_V - C_I$ [VNI]
N	$-\lambda C_I$ [NS]		$-C_I$ [NI]

The relative cost is defined as  $c = C_V/C_I$ . Generally, the cost of vaccination is less than the effective cost of infection, so we have  $0 < c < 1$ . For convenience, we redefine Eq. (3) as

$$\begin{cases} \pi_{VES} = -c \\ \pi_{VNS} = -c - \lambda \\ \pi_{VNI} = -c - 1 \\ \pi_{NS} = -\lambda \\ \pi_{NI} = -1 \end{cases} \quad (3)$$

When a susceptible individual adopts the IB-RA method, she selects a random neighbor to compare costs and payoffs and choose the most profitable strategy. It is assumed that she imitates her random neighbor's strategy with a probability given by the Fermi updating rule [66–68]. In particular, an individual belonging to the  $S_V$  compartment (hence with a VNS payoff) will imitate a random neighbor with NS or NI payoffs with probabilities:

$$P(VNS \leftarrow NS) = \frac{1}{1 + \exp[-(-\lambda - (-C_V - \lambda))/\kappa]} \quad (4)$$

$$P(VNS \leftarrow NI) = \frac{1}{1 + \exp[-(-C_I - (-C_V - \lambda))/\kappa]} \quad (5)$$

$$P(VNS \leftarrow VES) = \frac{1}{1 + \exp[-(-C_V - (-C_V - \lambda))/\kappa]} \quad (6)$$

Here, the parameter  $\kappa$  describes the degree of rationality of an individual: when  $\kappa$  is zero, the probability to switch to the lowest cost strategy is one (full rationality); in the large  $\kappa$  limit, the Fermi's probability is always 1/2 (random choice).

Analogously, an individual belonging to the  $S_N$  compartment (hence with a NS payoff) will imitate a random neighbor with VES, VNS, or VNI payoffs with probabilities:

$$P(NS \leftarrow VES) = \frac{1}{1 + \exp[-(-C_V - (-\lambda))/\kappa]} \quad (7)$$

$$P(NS \leftarrow VNS) = \frac{1}{1 + \exp[-(-C_V - \lambda - (-\lambda))/\kappa]} \quad (8)$$

$$P(NS \leftarrow VNI) = \frac{1}{1 + \exp[-(-C_V - C_I - (-\lambda))/\kappa]} \quad (9)$$

Now, we can finally write down the interaction terms  $\Delta_1$  and  $\Delta_2$  introduced in the dynamic system (1):

$$\begin{aligned} \Delta_1 &= S_N \cdot V_E P(NS \leftarrow VES) + S_N \cdot S_V P(NS \leftarrow VNS) + S_N \cdot I_V P(NS \leftarrow VNI) \\ &= S_N \cdot V_E \frac{1}{1 + \exp[-(-c - (-\lambda))/\kappa]} + \\ &\quad S_N \cdot S_V \frac{1}{1 + \exp[-(-c - \lambda - (-\lambda))/\kappa]} + \end{aligned} \quad (10)$$

$$S_N \cdot I_V \frac{1}{1 + \exp[-(-c - 1 - (-\lambda))/\kappa]}$$

$$\begin{aligned} \Delta_2 &= S_V \cdot S_N P(VNS \leftarrow NS) + S_V \cdot I_N P(VNS \leftarrow NI) \\ &= S_V \cdot S_N \frac{1}{1 + \exp[-(-\lambda_1 + \lambda_2) - (-c - \lambda)/\kappa]} + \\ &\quad S_V \cdot I_N \frac{1}{1 + \exp[-(-1 - (-c - \lambda))/\kappa]} \end{aligned} \quad (11)$$

### 2.2.2. Society-based risk assessment (SB-RA)

In the SB-RA case, individuals make their decisions based on the global average payoff, rather than the payoff of a randomly selected neighbor. The global average payoffs,  $\pi_C$  and  $\pi_D$ , of susceptible individuals adopting the cooperation and deception strategy, respectively, can be written as

$$\pi_C = \frac{V_E \cdot (-C_V) + S_V \cdot (-C_V - \lambda C_I) + I_V \cdot (-C_V - C_I)}{V_E + S_V + I_V} \quad (12)$$

$$\pi_D = \frac{S_N \cdot (-\lambda C_I) + I_N \cdot (-C_I)}{S_N + I_N} \quad (13)$$

Then, the Fermi's probability for an individual ineffectively vaccinated to switch to the deception strategy is

$$P(VNS \leftarrow D) = \frac{1}{1 + \exp[-(\pi_D - (-C_V - \lambda)) / \kappa]} \quad (14)$$

Instead, the Fermi's probability for a non-vaccinated individual to switch to the cooperation strategy is

$$P(NS \leftarrow C) = \frac{1}{1 + \exp[-(\pi_C - (-\lambda)) / \kappa]} \quad (15)$$

This time, the interaction terms are:

$$\Delta_1 = S_N \cdot (V_E + S_V + I_V) \cdot P(NS \leftarrow C) \quad (16)$$

$$\Delta_2 = S_V \cdot (S_N + I_N) \cdot P(VNS \leftarrow D) \quad (17)$$

### 3. Reproduction number

The reproduction number  $R_0$  is defined as the average number of infections caused by an infected person. If it is larger than 1 and no restrictive measures are applied, the epidemic will continue to grow. The greater  $R_0$ , the faster the epidemic spreads. When it is  $< 1$ , instead, the epidemic will gradually slow down or even disappear.

#### 3.1. Next-generation matrix method

Here, we briefly show the next-generation matrix method [69,70] to find the basic reproduction number  $R_0$ .

Step 1: Defining  $I = (I_V, I_N)^T$ , and dynamic system (1) can be written as

$$\frac{dI}{dt} = r(I) - h(I) \quad (18)$$

Where  $r(I)$  is the proportion matrix of newly infected individuals and  $h(I)$  is the transfer proportion matrix of newly recovered individuals.

$$r(I) = \begin{bmatrix} S_V \left[ 1 - (1 - \beta)^{\langle k \rangle (I_V + I_N)} \right] \\ S_N \left[ 1 - (1 - \beta)^{\langle k \rangle (I_V + I_N)} \right] \end{bmatrix} = \begin{bmatrix} r_1 \\ r_2 \end{bmatrix} \quad (19)$$

$$h(I) = \begin{bmatrix} \mu I_V \\ \mu I_N \end{bmatrix} = \begin{bmatrix} h_1 \\ h_2 \end{bmatrix} \quad (20)$$

Step 2: The disease-free equilibrium point of the dynamic system is  $E_0 = (S_N^*, S_V^*, I_N^*, I_V^*, V_E^*, R^*) = (1, 0, 0, 0, 0, 0)$ . The Jacobian  $F$  and  $V$  of the matrices  $r(I)$  and  $h(I)$  at the disease-free equilibrium point are

$$F = \left[ \frac{\partial r(I)}{\partial I} \right] \Big|_{E_0} = \begin{bmatrix} \frac{\partial r_1}{\partial I_V} & \frac{\partial r_1}{\partial I_N} \\ \frac{\partial r_2}{\partial I_V} & \frac{\partial r_2}{\partial I_N} \end{bmatrix} \Big|_{E_0}$$

$$= \begin{bmatrix} -S_V^* \langle k \rangle (1 - \beta)^{\langle k \rangle (I_V^* + I_N^*)} I_N (1 - \beta) & -S_V^* \langle k \rangle (1 - \beta)^{\langle k \rangle (I_V^* + I_N^*)} I_N (1 - \beta) \\ -S_N^* \langle k \rangle (1 - \beta)^{\langle k \rangle (I_V^* + I_N^*)} I_N (1 - \beta) & -S_N^* \langle k \rangle (1 - \beta)^{\langle k \rangle (I_V^* + I_N^*)} I_N (1 - \beta) \end{bmatrix} \Big|_{E_0}$$

$$= \begin{bmatrix} 0 & 0 \\ -\langle k \rangle I_N (1 - \beta) & -\langle k \rangle I_N (1 - \beta) \end{bmatrix} \quad (21)$$

$$V = \left[ \frac{\partial h(I)}{\partial I} \right] = \begin{bmatrix} \frac{\partial h_1}{\partial I_V} & \frac{\partial h_1}{\partial I_N} \\ \frac{\partial h_2}{\partial I_V} & \frac{\partial h_2}{\partial I_N} \end{bmatrix} = \begin{bmatrix} \mu & 0 \\ 0 & \mu \end{bmatrix} \quad (22)$$

Step 3: The basic reproduction number  $R_0$  of the dynamic system is the spectral radius of the matrix  $FV^{-1}$ , i.e., its largest eigenvalue:

$$R_0 = \rho(FV^{-1}) = \rho \left( \begin{bmatrix} 0 & 0 \\ \frac{-\langle k \rangle I_N (1 - \beta)}{\mu} & \frac{-\langle k \rangle I_N (1 - \beta)}{\mu} \end{bmatrix} \right) \quad (23)$$

$$= \max(\lambda_1^{FV^{-1}}, \lambda_2^{FV^{-1}}) = -\frac{\langle k \rangle I_N (1 - \beta)}{\mu}$$

#### 3.2. Effective reproduction number

The definition of  $R_0$  requires that all the people in the population are susceptible. The number of susceptible individuals decreases when the disease starts to spread and there are conditions for post-infection immunity or prevention and control measures. As a result, for the effective reproduction number  $R_e(t)$  calculation, the disease-free equilibrium is.

$$S_N^* = S_N(t), S_V^* = S_V(t), I_N^* = I_V^* = 0 \quad (24)$$

And the effective reproduction number  $R_e(t)$  at any time  $t$  is also given by the spectral radius of  $FV^{-1}$  which is the largest eigenvalue of  $FV^{-1}$  [3,71].

### 4. Numerical simulations

In this section, we show in details the numerical results of our coupled disease-vaccination behavior dynamic model defined by Eq. (1), both in the IB-RA and the SB-RA cases.

#### 4.1. Parameter influence on compartments dynamics

We first study the numerical solutions of the dynamical system in (1) and their dependence on the model parameters employing the Runge-Kutta method [15]. Fig. 2(a) shows the numerical solutions of Eq. (1) in the IB-RA case when the parameters are set to  $\beta = 0.3$ ,  $\mu = 0.3$ ,  $\kappa = 0.1$ ,  $e = 0.6$ ,  $\langle k \rangle = 4.2$ ,  $c = 0.1$ , and the initial conditions are  $(S_V(0), S_N(0), I_V(0), I_N(0), V_E(0), R) = (0.4999, 0.4999, 0.001, 0.001, 0, 0)$ . Here, it can be observed that the proportion of non-vaccinated susceptible individuals increases at an early stage, and then decreases. This is explained as follows. At the beginning of the epidemic, the proportion of infected individuals in the network is small and therefore the risk of infection for susceptible individuals is low. Hence, in this phase, the non-vaccination strategy is the optimal strategy. This will result in the rapid spread of the disease. In the second phase, the risk of infection among susceptible individuals in the network increases as the disease spreads.

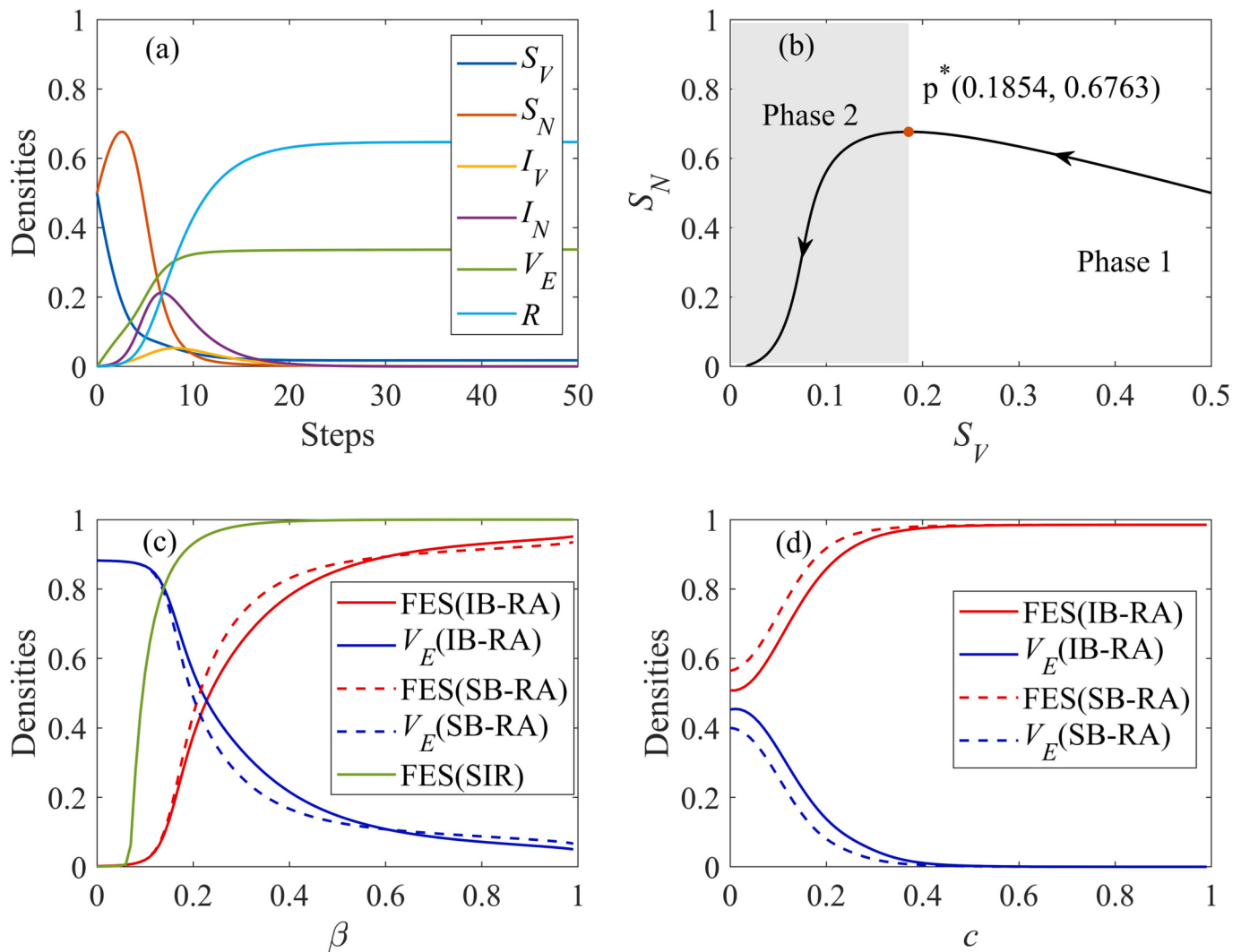


**Fig. 2.** Numerical simulations of the model. (a) Temporal evolution of epidemic states in the IB-RA case. (b) Evolutionary phase space of  $S_V$  and  $S_N$  states in the IB-RA case. (c) Final epidemic size and vaccination coverage vs  $\beta$ , for the IB-RA and SB-RA cases. These are compared with the final epidemic scale of the SIR model. (d) Final epidemic size and vaccination coverage vs  $c$ , for the IB-RA and SB-RA cases.

The risk perception of susceptible individuals who do not vaccinate gradually becomes larger than the cost of vaccination, making the vaccination strategy more profitable.

To better emphasize this point, Fig. 2(b) shows the dynamic phase diagram between non-vaccinated susceptible individuals ( $S_N$ ) and vaccinated susceptible individuals ( $S_V$ ), still in the IB-RA case. In phase 1, the average risk of infection is low for susceptible people. In this region, the non-vaccination strategy is preferred. In phase 2, the average risk of infection for susceptible people is higher and the vaccination strategy prevails. With the above parameters, the coordinates of the tipping point between the two phases are  $p^*(0.1854, 0.6763)$ .

The final epidemic size (FES) and the corresponding vaccination coverage ( $V_E$ ) as a function of  $\beta$  are shown in Fig. 2(c). Here, the FES of the IB-RA and SB-RA cases is compared with that of the classical SIR model. From this comparison, it is evident that, as expected, vaccination can effectively reduce the total number of infections in the population. Moreover, when  $\beta$  is small, the final epidemic size in the IB-RA case is smaller and the vaccination coverage is larger than those in the SB-RA case. On the contrary, when  $\beta$  is larger, the SB-RA case has a smaller final epidemic size and a larger vaccination coverage than those in the IB-RA case. Remarkably, this implies that, when the disease breaks out, the population should share as much information as possible so that susceptible individuals can adopt a global updating rule and reduce the

total number of infections.

Finally, Fig. 2(d) shows the final epidemic size and the corresponding vaccination coverage as a function of  $c$ . We see that, in both cases,  $V_E$  is a decreasing function of  $c$ , while the FES is an increasing function. Also, the FES in the IB-RA case is smaller than that in the SB-RA case, particularly for small values of  $c$ . Hence, the relative cost  $c$  has a greater impact in the SB-RA case and, for small relative cost, the IB-RA updating rule is better for controlling the disease spreading.

#### 4.2. Phase diagrams of the final epidemic size

To further understand the impact of evolving strategies on the spread of the disease, we now show various phase diagrams of the FES in different parameter spaces. In the following, when the average degree  $\langle k \rangle$  is not a variable parameter of the phase diagram, it is set to 4.2 or 7.6. The smaller of these two values represents the situation where restrictive measures are applied to control the outbreak (e.g., quarantine); the larger value, instead, is more suitable for the case where no restrictions are applied, as shown in [3].

In Fig. 3, we show the FES phase diagrams versus recovery rate ( $\mu$ ) and per-contact transmission probability ( $\beta$ ). Fig. 3(a-d) are in the IB-RA case, while Fig. 3(e-h) are in the SB-RA case. Comparing the upper panels with the lower ones, we observe that, when restrictive measures

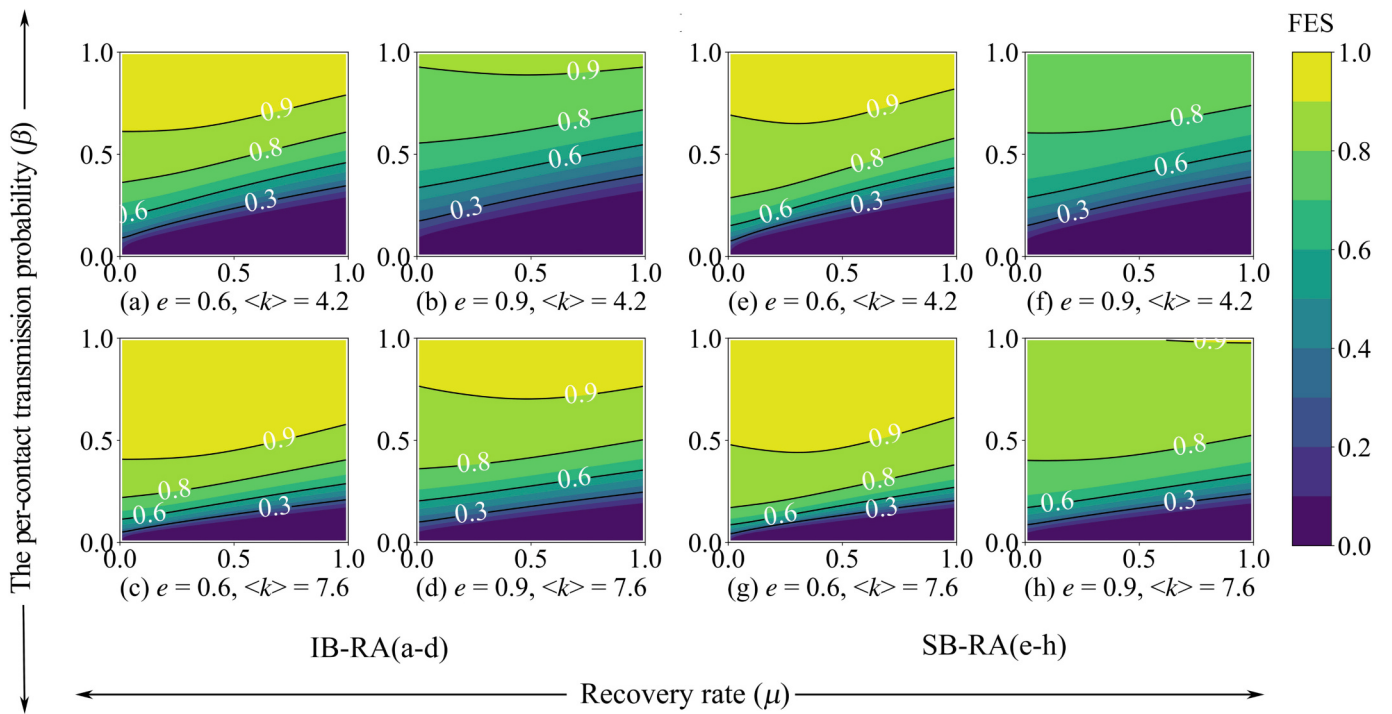


**Fig. 3.** FES Phase diagrams with respect to recovery rate and per-contact transmission probability with  $e = 0.6$  or  $0.9$ ,  $\langle k \rangle = 4.2$  or  $7.6$ . Panel a-d: IB-RA case. Panel e-h: SB-RA case.

are applied (lower  $\langle k \rangle$ ), the regions corresponding to high FES (shown in yellow) shrinks. Hence, as already well known, the total number of infections can be effectively controlled by supervising the number of interactions in the population. In addition, higher recovery rate and vaccination efficacy also reduce the FES. Notably, the latter effect is more pronounced in the SB-RA case. In general, for any combination of  $\mu$  and  $\beta$ , the FES in the SB-RA diagrams is smaller than that in the IB-RA

diagrams. This again suggests that having more information about payoffs in society and adopting a global strategy are more favorable to reducing infections in the population. In Fig. 9 in Appendix A, the phase diagram of  $V_E$  against the same parameters of Fig. 3 is shown. Here, one can observe that high values of  $\mu$  and low values of  $\beta$  increase the number of (effectively) vaccinated individuals.

The phase diagrams of the FES versus relative cost ( $c$ ) and per-

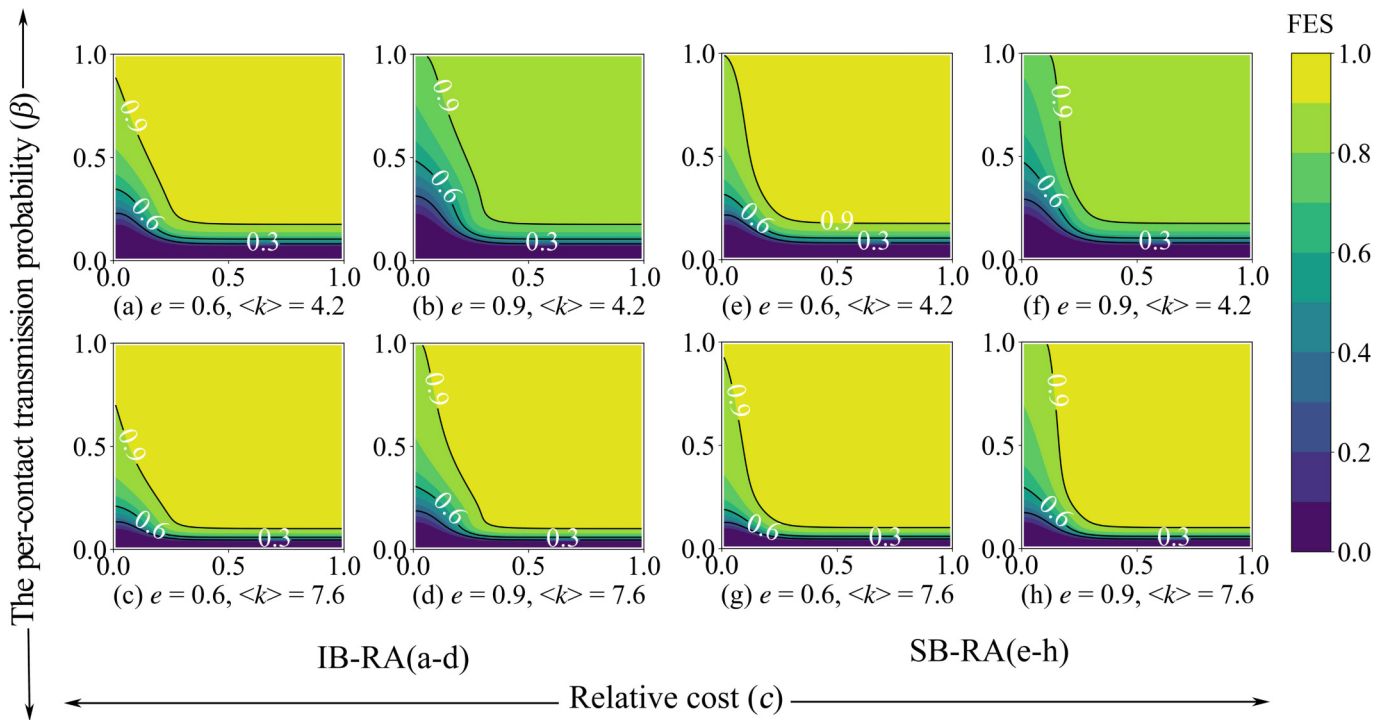


**Fig. 4.** FES Phase diagrams with respect to relative cost and per-contact transmission probability with  $e = 0.6$  or  $0.9$ ,  $\langle k \rangle = 4.2$  or  $7.6$ . Panel a-d: IB-RA case. Panel e-h: SB-RA case.

contact transmission probability ( $\beta$ ) are shown in Fig. 4. When  $\beta$  is small, the FES goes to zero for any value of  $c$ . On the other hand, when  $\beta$  is large, the FES gradually increases with the relative cost (consistently with Fig. 2(d)). It is also observed in Fig. 10 of Appendix A that increasing the cost of vaccination prevents the spread of the cooperative (pro-vaccination) strategy. Note that when  $c$  is small, the IB-RA method favors a higher vaccination coverage than the SB-RA method.

Finally, the phase diagrams of the FES versus average degree ( $\langle k \rangle$ ) and vaccination efficacy ( $e$ ) are shown in Fig. 5. In Fig. 11 in Appendix A are shown the phase diagrams of  $V_E$  versus the same parameters. Here, we observe that a lower average degree and higher vaccination efficacy can reduce FES and increase  $V_E$ .

#### 4.3. Effect of time delay on the epidemic spreading

In reality, there is a time delay between an individual's implementation of any vaccination strategy and the observation of virus spread. This delay is due, for example, to the thinking time about which strategy to adopt or simply to the bureaucratic time between booking the vaccine and its execution. In this section, we slightly modify our model to account for this time lag and observe how unvaccinated susceptible individuals and the final epidemic size vary as this time lag varies.

Let us denote by  $\tau$  the lag time between the spread of infection and the spread of vaccination behavior. The ordinary differential equations of system (1) are thus transformed into delay differential equations (DDE). The form of the DDE is the same as in system (1), except that the interaction terms are modified as follows:

$$\Delta_1 = S_N(t - \tau) \cdot V_E(t - \tau)P(NS \leftarrow VES) + S_N(t - \tau) \cdot S_V(t - \tau)P(NS \leftarrow VNS) + S_N(t - \tau) \cdot I_V(t - \tau)P(NS \leftarrow VNI)$$

$$\Delta_2 = S_V(t - \tau) \cdot S_N(t - \tau)P(VNS \leftarrow NS) + S_V(t - \tau) \cdot I_N(t - \tau)P(VNS \leftarrow NI)$$

The solution of this DDE system is shown in Fig. 6, where we set the model parameters as those in Fig. 2.

From Fig. 6(a), we observe that, as  $\tau$  increases, more individuals choose the non-vaccination strategy. In particular, the peak of  $S_N$

increases and moves forward in time. Fig. 6(b) shows the behavior of the FES when  $\tau$  increases. We note that, when  $\tau < 3$ , the FES is small, but that of the SB-RA case is slightly larger than that of the IB-RA case. When  $\tau$  increases, also the FES increases, but that of the IB-RA case becomes significantly larger than that of the SB-RA case. This difference continues to grow until a saturation point ( $\tau \approx 5$ ) where the FES in both cases reach its maximum value (where most of the population has been infected).

These results suggest that to control the virus spreading it is necessary to reduce the time delay for vaccine execution. If this is not possible, adopting a global viewpoint for deciding the vaccination behavior strategy limits the negative effects of time delay compared with adopting an individual viewpoint. In general, early promotion of vaccination strategy can effectively reduce the infection size of the population.

#### 5. Model validation with data of COVID-19 in France

To validate our model, real data from the COVID-19 pandemic in France is analyzed. Since there is no data on people's behavior and vaccination strategies, we restrict ourselves from comparing real data with our mechanism of disease spreading. In this section, a time-varying per-contact transmission probability  $\beta$  is considered.

##### 5.1. Data acquisition and preprocessing

Our data come from the Our World in Data and COVID-19 data archive of the Center for Systems Science and Engineering (CSSE) at Johns Hopkins University (JHU) [3,72].

The LOWESS (locally weighted regression scatterplot smoothing) method is used to smooth the data. LOWESS is a nonparametric method for local regression analysis [73,74]. It divides the samples into small intervals and performs polynomial fitting on each interval. This process is repeated to obtain weighted regression curves in different intervals. Finally, the centers of these regression lines are connected to form a complete regression curve.

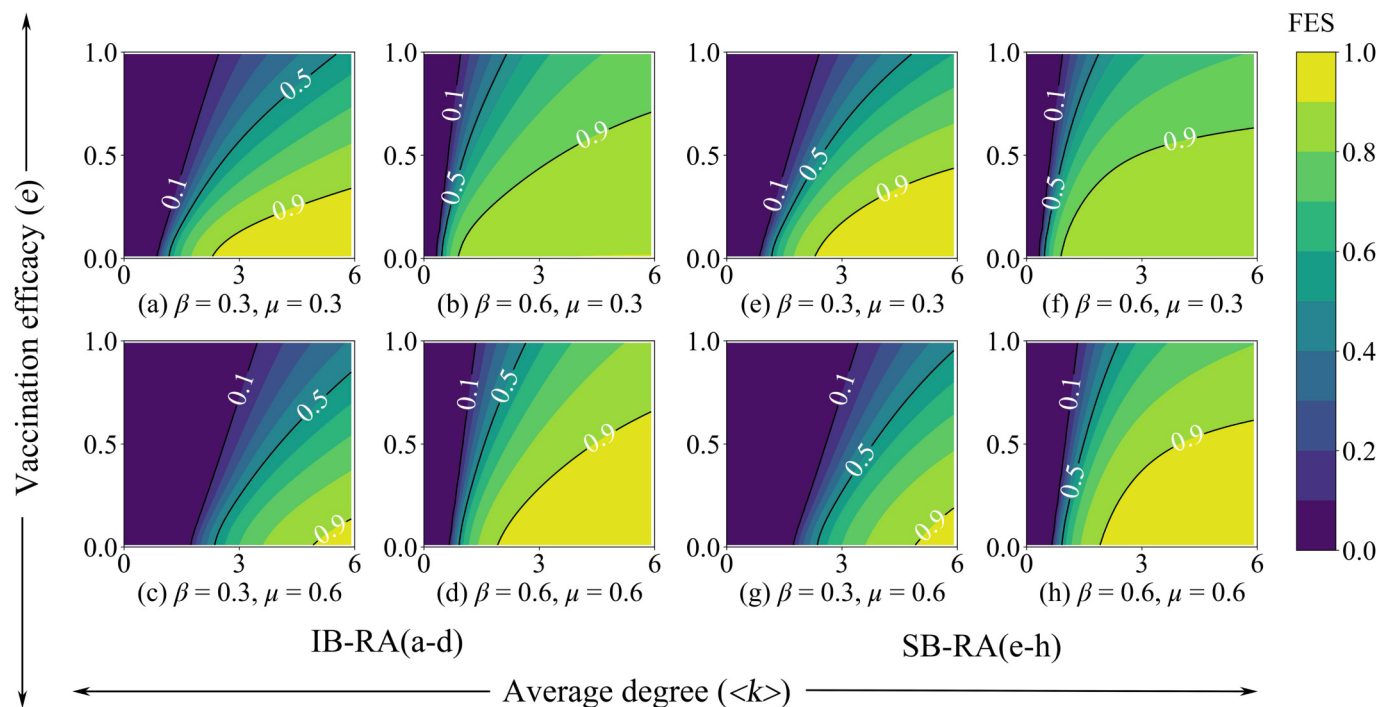


**Fig. 5.** FES Phase diagrams with respect to average degree and vaccination effectiveness with  $\beta = 0.3$  or  $0.6$ ,  $\mu = 0.3$  or  $0.6$ . Panel a-d: IB-RA case. Panel e-h: SB-RA case.

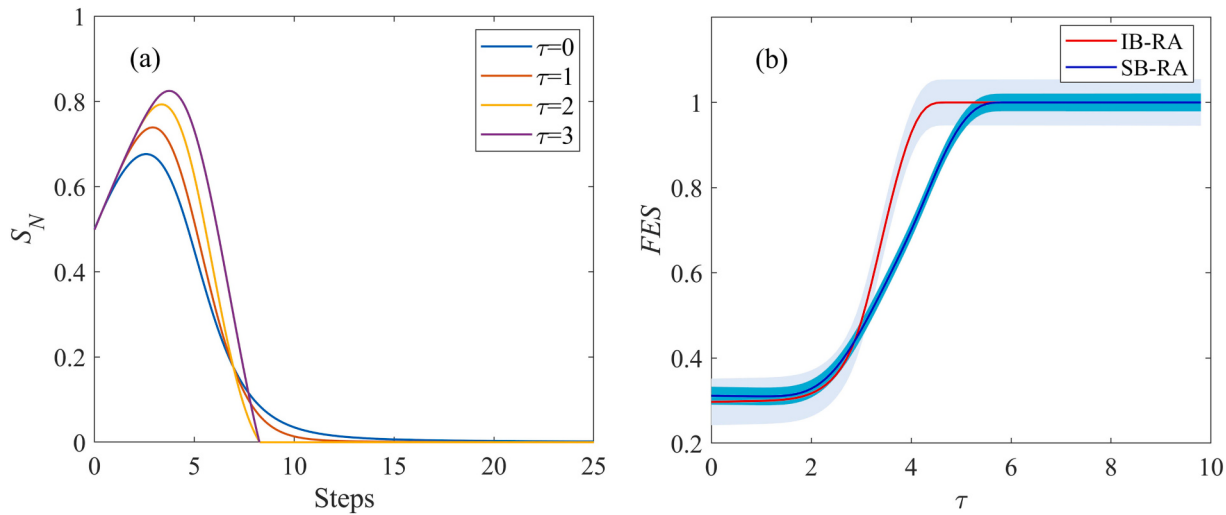


**Fig. 6.** Effect of time delay on the epidemic spreading. (a) Temporal evolution of susceptible non-vaccinated individuals in the IB-RA case for different values of time delay. (b) Final epidemic size vs time delay in the IB-RA and SB-RA cases.

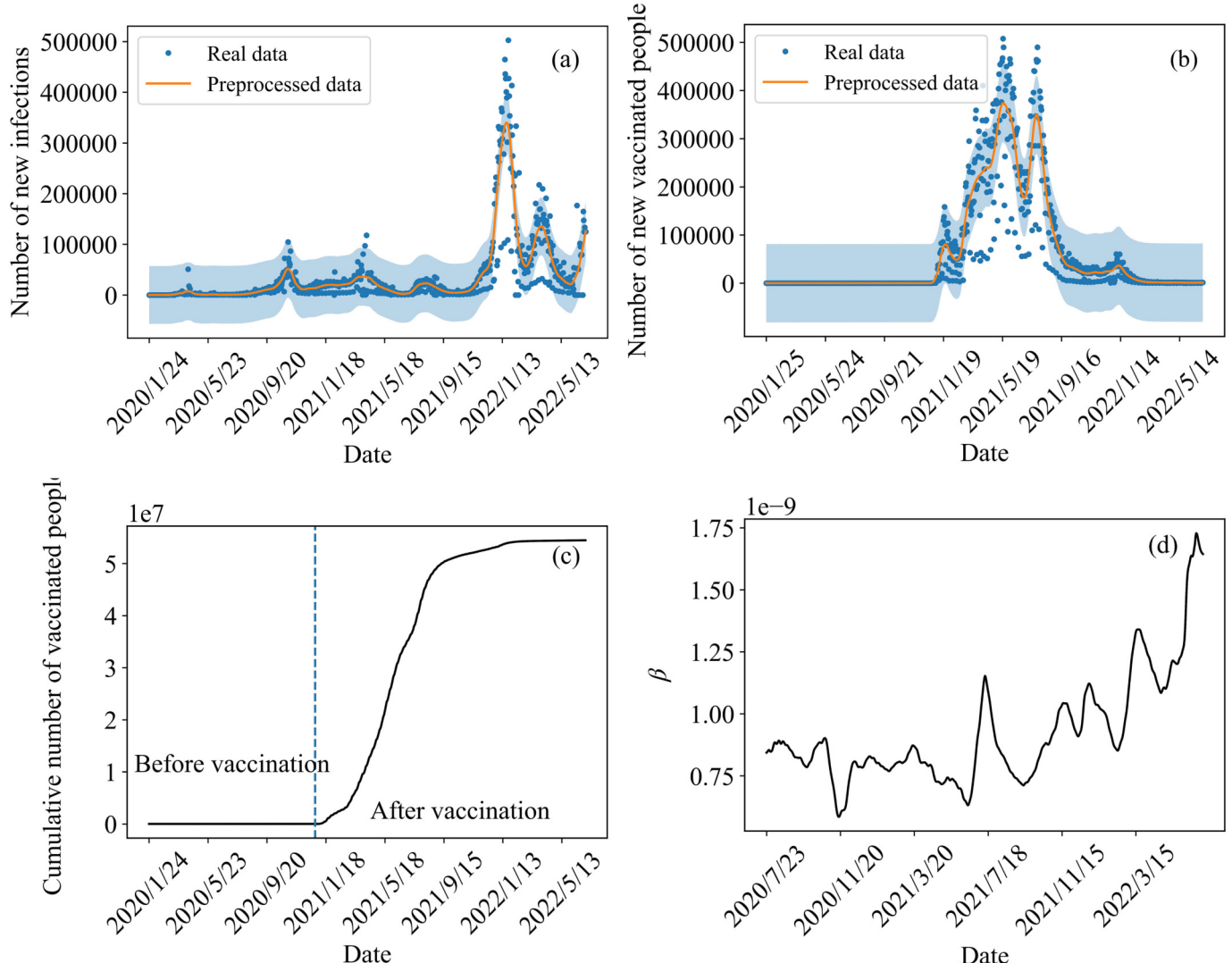


**Fig. 7.** Analysis of the COVID-19 epidemic data in France from January 24, 2020 to July 2, 2022. (a) Temporal evolution of new infections. (b) Temporal evolution of newly vaccinated people. (c) Temporal evolution of the cumulative number of vaccinated people. (d) Temporal evolution of the per-contact transmission probability computed combining real data with Eq. (29).

## 5.2. Parameters fitting

Let us denote by  $H(t)$  the proportion of health individuals in the population who are not infected, i.e.,  $H(t) = S_N(t) + S_V(t) + V_E(t)$ , by  $S(t)$  the proportion of susceptible individuals, i.e.,  $S(t) = S_N(t) + S_V(t)$ , and by  $I(t)$  the proportion of infected individuals, i.e.,  $I(t) = I_V(t) + I_N(t)$ . The dynamic system in Eq. (1) can be rewritten as

$$\begin{cases} \frac{dH(t)}{dt} = -S(t) \left[ 1 - (1 - \beta_t)^{\langle k \rangle I(t)} \right] \\ \frac{dI(t)}{dt} = S(t) \left[ 1 - (1 - \beta_t)^{\langle k \rangle I(t)} \right] - \mu I(t) \\ \frac{dR(t)}{dt} = \mu I(t) \end{cases} \quad (25)$$

Since the real data describes the number of health, infected, and recovered individuals per day, we discretize the above differential equations:

$$\begin{cases} H(t+1) - H(t) = -S(t) \left[ 1 - (1 - \beta_t)^{\langle k \rangle I(t)} \right] \\ I(t+1) - I(t) = S(t) \left[ 1 - (1 - \beta_t)^{\langle k \rangle I(t)} \right] - \mu I(t) \\ R(t+1) - R(t) = \mu I(t) \end{cases} \quad (26)$$

Noting that

$$H(t+1) - H(t) + I(t+1) - I(t) + R(t+1) - R(t) = 0 \quad (27)$$

we can write the following relations

$$\mu = \frac{R(t+1) - R(t)}{I(t)} \quad (28)$$

$$\beta_t = 1 - \exp \left( \frac{\ln \left[ 1 - \frac{I(t+1) - I(t) + R(t+1) - R(t)}{S(t)} \right]}{\langle k \rangle I(t)} \right) \quad (29)$$

The daily number of new infections and newly vaccinated people in France from January 24, 2020, to July 2, 2022, is shown in Fig. 7(a-b). The measured parameters are  $e = 0.75$ ,  $\mu = 0.3$  and  $\langle k \rangle = 6$  [61]. Solid

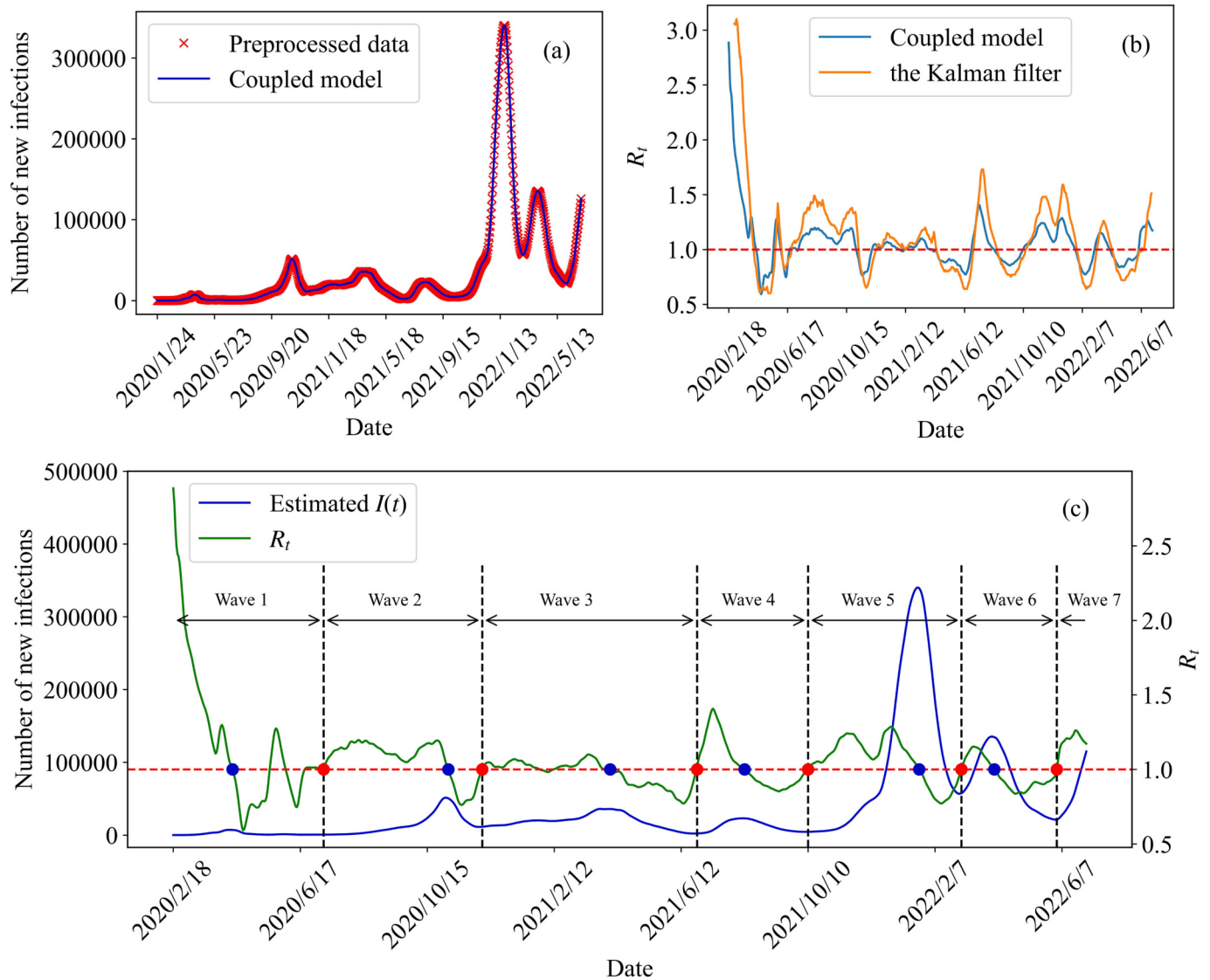


**Fig. 8.** Comparison of empirical data with our couple disease-vaccination behavior dynamic. (a) Temporal evolution of new infections. (b) Temporal evolution of the effective reproduction number. (c) Temporal evolution of new infections and effective reproduction number. Time is divided in seven intervals, each corresponding to a new epidemic wave.

lines represent smoothed data and shaded areas are the 95 % confidence intervals. The cumulative number of vaccinated people is shown in Fig. 7(c). On October 27, 2022, the population in France began to be gradually vaccinated. Fig. 7(d) shows the per-contact transmission probability as a function of time, obtained by applying data to Eq. (29).

### 5.3. Reproduction number analysis

The above fitting of COVID-19 pandemic data is used to calculate the effective reproduction number of the coupled disease-vaccination dynamic in France. By knowing the effective reproduction number, the pandemic outbreak can be prevented. In this section, we compare our coupled model with the Kalman filter method [75] applied to the data to calculate the effective reproduction number.

Fig. 8(a) shows the fitted time dependence of newly infected people calculated with our model using parameter  $\beta$  of Fig. 7(d), compared with smoothed data. The mean square error (MSE) between the two curves is calculated as follows:

$$MSE = \frac{1}{n} \sum_{i=1}^n (I(t) - \hat{I}(t))^2 \quad (30)$$

The MSE is equal to 0.00067, meaning that parameter  $\beta$  calculated with our model is reliable. In Fig. 8(b), the temporal behavior of the effective reproduction number predicted by our coupled model (with Eq. (23) and the same  $\beta$  of Fig. 7(d)) is compared with that obtained by the Kalman filter method. Remarkably, the two curves are very close to each other.

In Fig. 8(c), the green line represents the temporal behavior of the effective reproduction number computed with our model, while the blue line represents the temporal behavior of newly infected people. The spread of the pandemic is divided into seven intervals characterized by an epidemic wave, as shown in Table 3. Between intervals, the effective reproduction number is 1 and is marked by a red dot. After these points, the effective reproduction number will increase becoming larger than 1. The red dots, therefore, indicate the bottom of each previous epidemic wave and the probable outbreak of a new wave. On the other hand, after the blue dots, the effective reproduction number will decrease becoming  $<1$ . This indicates that the epidemic will gradually decrease. Together, these results suggest a method to give an early warning of the epidemic outbreak.

## 6. Conclusion and discussion

To summarize, a dynamic model of coupled disease-vaccination behavior is introduced to investigate the impact of individual vaccination strategies evolution on the spread of infectious diseases. In our model, the mechanism of disease spreading is described by an infectious disease transmission model based on the mean-field approximation theory. It is assumed that interactions between individuals occur in a homogeneous social network, and the infection rate is nonlinear with the number of neighbors in the network and describes simultaneous contacts. This mechanism is combined with an individual decision-making process for determining whether to vaccinate or not. It is described by a model of vaccination strategy evolution based on the evolutionary game theory. In this framework, individuals decide whether to change their vaccination strategy from a cost-benefit analysis. We considered two individual vaccination strategy updating rules: a local one, based on a comparison with the payoff of a single random neighbor; a global one, based on a comparison with the average payoff of society. Unlike previous studies [34,63,64], our model treats the vaccination strategy and disease dynamics as interrelated mechanisms that evolve simultaneously and give rise to a unique process. To validate our infection transmission model, we analyzed the real data from the COVID-19 pandemic in France.

Our findings suggest that adopting a global point of view for

**Table 3**

Seven waves of the COVID-19 pandemic outbreak in France from January 24, 2020 to July 2, 2022.

Wave No.	Starting time	End Time	Change point
1	January 24, 2020	July 9, 2020	$R_{09/07/2020} = 0$
2	July 9, 2020	December 6, 2020	$R_{06/12/2020} = 0$
3	December 6, 2020	June 27, 2021	$R_{27/06/2021} = 0$
4	June 27, 2021	October 10, 2021	$R_{10/10/2021} = 0$
5	October 10, 2021	March 4, 2022	$R_{04/03/2022} = 0$
6	March 4, 2022	June 2, 2022	$R_{02/06/2022} = 0$
7	June 2, 2022	July 2, 2022	

updating the individual vaccination strategy is better for reducing the final epidemic size. Hence, it is beneficial to share as much information with as many people as possible to encourage behaviors based on adopting a global updating strategy. The numerical simulations show that the proportion of susceptible individuals who do not vaccinate increases at an early stage and then decreases. This is a consequence of the temporal behavior of the individual risk perception of infection produced by the model. Furthermore, our analyses confirm that restrictive measures to reduce the average number of interactions in the population are effective in decreasing the final epidemic size. Finally, analyzing the real data of COVID-19, we show an early warning method for new epidemic waves. Quantitative analysis of all these factors can better guide policy makers' decisions.

Overall, our model can better describe the co-evolution between the infection spreading and the vaccination process for highly infectious and rapidly spreading viruses, such as COVID-19. However, our work can be extended and improved in several ways. For example, one possible direction is to consider the vaccination process split into multiple vaccinations, similarly to some vaccination protocols for COVID-19. Furthermore, it is possible to study the situation where vaccine efficacy decreases over time, as usual in real cases. Also, it is possible to study the behavioral effects of other protective measures (wearing a face mask, washing hands, social distancing, etc.) that have less impact, in terms of payoff, than vaccination. Regarding data collection and model validation, it would be important to design a method to detect people's vaccination behaviors and strategies during pandemics.

## CRediT authorship contribution statement

Xueyu Meng: Conceptualization, Methodology, Formal analysis, Writing - original draft. Jianhong Lin: Data curation, Validation. Yufei Fan: Methodology, Writing – review. Fujuan Gao: Conceptualization, Methodology. Enrico Maria Fenolaltea: Methodology, Writing - review & editing. Zhiqiang Cai: Methodology, Supervision. Shubin Si: Conceptualization, Formal analysis.

## Declaration of competing interest

The authors declare that they have no known competing financial interests or personal relationships that could have appeared to influence the work reported in this paper.

## Data availability

No data was used for the research described in the article.

## Acknowledgments

The authors would like to thank Ruijie Wang who supported this work with relevant discussions, and Alejandro Lage Castellanos who helped in the writing phase. The authors gratefully acknowledge the financial supports for this research from the National Natural Science Foundation of China (Nos. 72271200, 71871181 and 72231008), the

111 Project (No. B13044), the National Foreign Expert Project of the Ministry of Science and Technology of China (No. G2021183007L), the Key R&D Program of Shaanxi Province (No. 2022KW-15) and the

Innovation Foundation for Doctor Dissertation of Northwestern Polytechnical University (No. CX2022040).

#### Appendix A. $V_E$ phase diagrams with game theory approach for different parameters

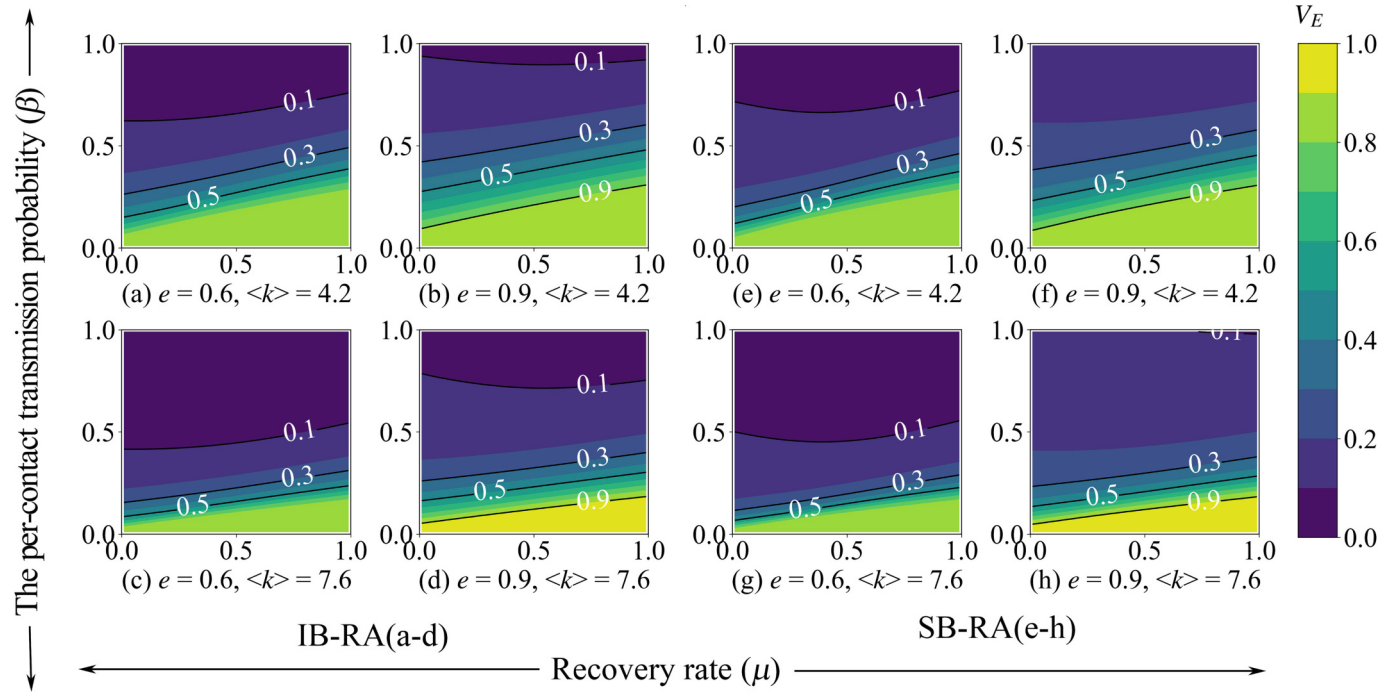


**Fig. 9.**  $V_E$  phase diagrams with respect to recovery rate and per-contact transmission probability with  $e = 0.6$  or  $0.9$ ,  $\langle k \rangle = 4.2$  or  $7.6$ . Panel a-d: IB-RA case. Panel e-h: SB-RA case.

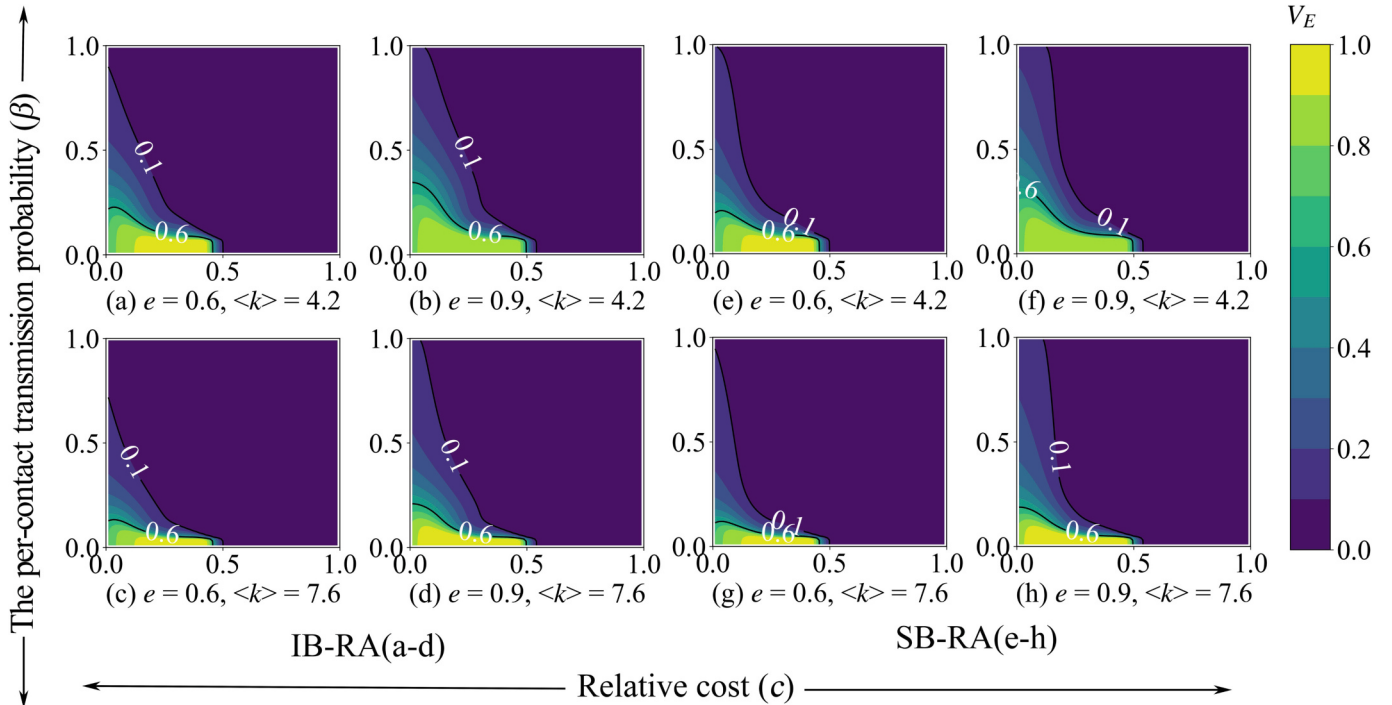


**Fig. 10.**  $V_E$  phase diagrams with respect to relative cost and per-contact transmission probability with  $e = 0.6$  or  $0.9$ ,  $\langle k \rangle = 4.2$  or  $7.6$ . Panel a-d: IB-RA case. Panel e-h: SB-RA case.

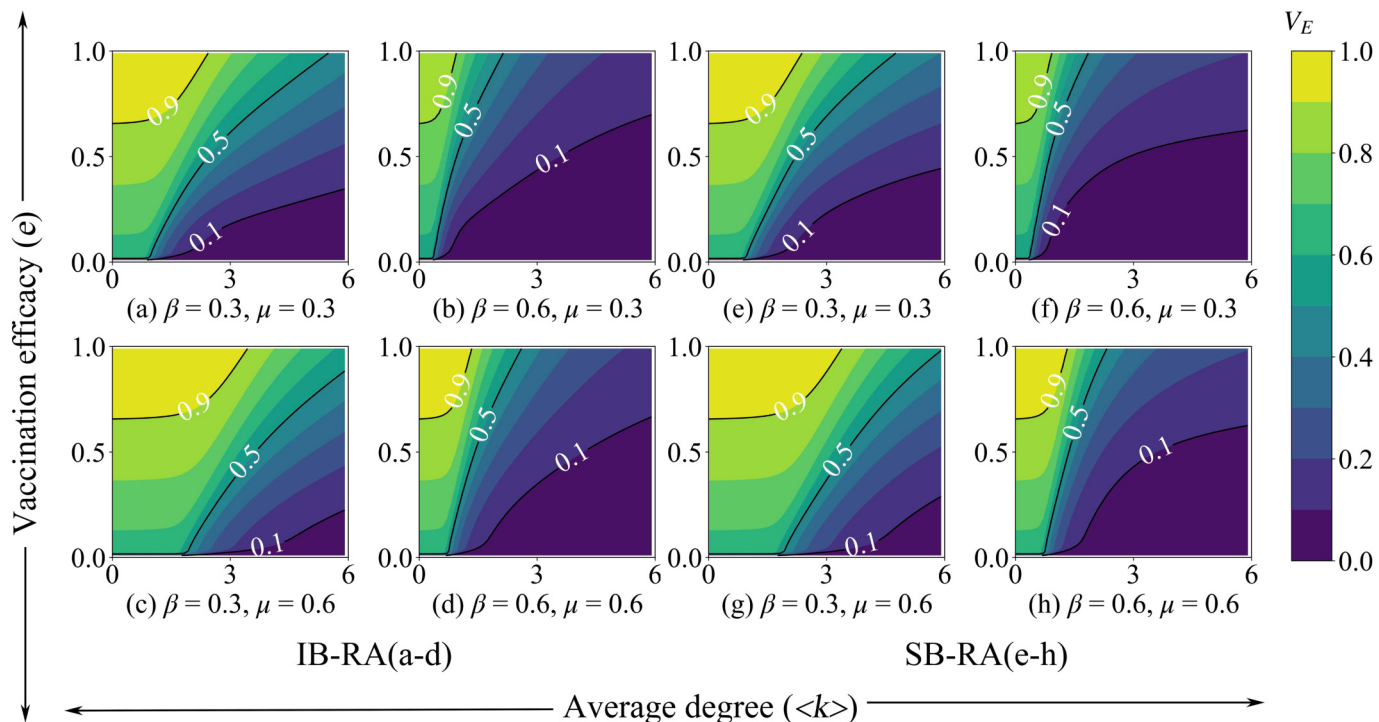


**Fig. 11.**  $V_E$  phase diagrams with respect to average degree and vaccination effectiveness with  $\beta = 0.3$  or  $0.6, \mu = 0.3$  or  $0.6$ . Panel a-d: IB-RA case. Panel e-h: SB-RA case.

## References

- [1] Aleta A, Martin-Coral D, Pastore YPA, Ajelli M, Litvinova M, Chinazzi M, et al. Modelling the impact of testing, contact tracing and household quarantine on second waves of COVID-19. *Nat Hum Behav* 2020;4:964–71. <https://doi.org/10.1038/s41562-020-0931-9>.
- [2] Goncalves ADS, Fernandes LHS, Nascimento ADC. Dynamics diagnosis of the COVID-19 deaths using the Pearson diagram. *Chaos Solitons Fractals* 2022;164: 112634. <https://doi.org/10.1016/j.chaos.2022.112634>.
- [3] Viana J, van Dorp CH, Nunes A, Gomes MC, van Boven M, Kretzschmar ME, et al. Controlling the pandemic during the SARS-CoV-2 vaccination rollout. *Nat Commun* 2021;12:3674. <https://doi.org/10.1038/s41467-021-23938-8>.
- [4] Wang Z, Andrews MA, Wu ZX, Wang L, Bauch CT. Coupled disease-behavior dynamics on complex networks: a review. *Phys Life Rev* 2015;15:1–29. <https://doi.org/10.1016/j.plrev.2015.07.006>.
- [5] Colizza V, Vespignani A. Invasion threshold in heterogeneous metapopulation networks. *Phys Rev Lett* 2007;99:148701. <https://doi.org/10.1103/PhysRevLett.99.148701>.
- [6] Kermack WO, McKendrick AG. A contribution to the mathematical theory of epidemics. *Proc. R. Soc. A: Math. Phys. Eng. Sci.* 1927;72:700–21. <https://doi.org/10.1088/rspa.1927.0118>.
- [7] Saeedian M, Khalighi M, Azimi-Tafreshi N, Jafari GR, Ausloos M. Memory effects on epidemic evolution: the susceptible-infected-recovered epidemic model. *Phys Rev E* 2017;95:022409. <https://doi.org/10.1103/PhysRevE.95.022409>.
- [8] Wei W, Xu W, Song Y, Liu J. Bifurcation and basin stability of an SIR epidemic model with limited medical resources and switching noise. *Chaos, Solitons Fractals* 2021;152. <https://doi.org/10.1016/j.chaos.2021.111423>.
- [9] Buldu JM, Antequera DR, Aguirre J. The resumption of sports competitions after COVID-19 lockdown: the case of the Spanish football league. *Chaos Solitons Fractals*. 2020;138:109964. <https://doi.org/10.1016/j.chaos.2020.109964>.
- [10] Gabrici EC, Protachevicz PR, Batista AM, Iarosc KC, de Souza SLT, Almeida ACL, et al. Effect of two vaccine doses in the SEIR epidemic model using a stochastic cellular automaton. *Physica A* 2022;597. <https://doi.org/10.1016/j.physa.2022.127258>.
- [11] Kokurin MM, Kokurin MY, Semenova AV. Iteratively regularized Gauss-Newton type methods for approximating quasi-solutions of irregular nonlinear operator equations in Hilbert space with an application to COVID-19 epidemic dynamics. *Appl Math Comput* 2022;431:127312. <https://doi.org/10.1016/j.amc.2022.127312>.
- [12] Zou R, Deng Z, Lu Y, Hu J, Han Z. Study of spreading phenomenon in network population considering heterogeneous property. *Chaos, Solitons Fractals* 2021;153. <https://doi.org/10.1016/j.chaos.2021.111520>.
- [13] Andreasen V. The final size of an epidemic and its relation to the basic reproduction number. *Bull Math Biol* 2011;73:2305–21. <https://doi.org/10.1007/s11538-010-9623-3>.
- [14] Keeling MJ, Eames KT. Networks and epidemic models. *J R Soc Interface* 2005;2: 295–307. <https://doi.org/10.1098/rsif.2005.0051>.
- [15] Mandal M, Jana S, Nandi SK, Khatua A, Adak S, Kar TK. A model based study on the dynamics of COVID-19: prediction and control. *Chaos Solitons Fractals* 2020; 136:109889. <https://doi.org/10.1016/j.chaos.2020.109889>.
- [16] Locatelli I, Trachsel B, Rousson V. Estimating the basic reproduction number for COVID-19 in Western Europe. *PLoS One*. 2021;16:e0248731. <https://doi.org/10.1371/journal.pone.0248731>.
- [17] Dai X, Li X, Guo H, Jia D, Perc M, Manshour P, et al. Discontinuous transitions and rhythmic states in the D-dimensional Kuramoto model induced by a positive feedback with the global order parameter. *Phys Rev Lett* 2020;125:194101. <https://doi.org/10.1103/PhysRevLett.125.194101>.
- [18] Gao S, Dai X, Wang L, Perra N, Wang Z. Epidemic spreading in metapopulation networks coupled with awareness propagation. *IEEE Trans Cybern* 2022;PP. <https://doi.org/10.1109/TCYB.2022.3198732>.
- [19] Khan MM, Arefin MR, Tanimoto J. Investigating the trade-off between self-quarantine and forced quarantine provisions to control an epidemic: an evolutionary approach. *Appl Math Comput* 2022;432:127365. <https://doi.org/10.1016/j.amc.2022.127365>.
- [20] Meng X, Han S, Wu L, Si S, Cai Z. Analysis of epidemic vaccination strategies by node importance and evolutionary game on complex networks. *Reliab Eng Syst Saf* 2022;219. <https://doi.org/10.1016/j.ress.2021.108256>.
- [21] Duan D, Lv C, Si S, Wang Z, Li D, Gao J, et al. Universal behavior of cascading failures in interdependent networks. *Proc Natl Acad Sci U S A* 2019;116:22452–7. <https://doi.org/10.1073/pnas.1904421116>.
- [22] Dui H, Meng X, Xiao H, Guo J. Analysis of the cascading failure for scale-free networks based on a multi-strategy evolutionary game. *Reliab Eng Syst Saf* 2020; 199. <https://doi.org/10.1016/j.ress.2020.106919>.
- [23] Ma C, Wang W, Cai Z, Zhao J. Maintenance optimization of reconfigurable systems based on multi-objective birnbaum importance. *Proc Inst Mech Eng O: J Risk Reliab* 2020;236:277–89. <https://doi.org/10.1177/1748006x20901983>.
- [24] Watts DJ, Strogatz SH. Collective dynamics of ‘small-world’ networks. *Nature* 1998;393:440–2. <https://doi.org/10.1038/30918>.
- [25] Barabasi A-Ls, Albert R. Emergence of scaling in random networks. *Science* 1999; 286:509–12. <https://doi.org/10.1126/science.286.5439.509>.
- [26] Pastor-Satorras R, Vespignani A. Epidemic spreading in scale-free networks. *Phys Rev Lett* 2001;86:3200–3. <https://doi.org/10.1103/PhysRevLett.86.3200>.
- [27] Pastor-Satorras R, Vespignani A. Epidemic dynamics in finite size scale-free networks. *Phys Rev E Stat Nonlin Soft Matter Phys* 2002;65:035108. <https://doi.org/10.1103/PhysRevE.65.035108>.
- [28] Newman ME. Spread of epidemic disease on networks. *Phys Rev E Stat Nonlin Soft Matter Phys* 2002;66:016128. <https://doi.org/10.1103/PhysRevE.66.016128>.
- [29] Wang Y, Chakrabarti D, Wang C, Faloutsos C. Epidemic spreading in real networks: an eigenvalue viewpoint. In: International symposium on reliable distributed systems. 10; 2003. p. 25–43. <https://doi.org/10.1109/RELDIS.2003.1238052>.

- [30] Zhu P, Wang X, Zhi Q, Ma J, Guo Y. Analysis of epidemic spreading process in multi-communities. *Chaos, Solitons Fractals*. 2018;109:231–7. <https://doi.org/10.1016/j.chaos.2018.02.007>.
- [31] Zhu P, Zhi Q, Guo Y, Wang Z. Analysis of epidemic spreading process in adaptive networks. *IEEE TRANSACTIONS ON CIRCUITS AND SYSTEMS—II: EXPRESS BRIEFS* 2019;66:1252–6. <https://doi.org/10.1109/TCSII.2018.2877406>.
- [32] Zhu P, Wang X, Li S, Guo Y, Wang Z. Investigation of epidemic spreading process on multiplex networks by incorporating fatal properties. *Appl Math Comput* 2019; 359:512–24. <https://doi.org/10.1016/j.amc.2019.02.049>.
- [33] Gao S, Chang L, Wang X, Liu C, Li X, Wang Z. Cross-diffusion on multiplex networks. *New J Phys* 2020;20:053047. <https://doi.org/10.1088/1367-2630/ab825e>.
- [34] Kabir KMA, Tanimoto J. Dynamical behaviors for vaccination can suppress infectious disease—a game theoretical approach. *Chaos, Solitons Fractals*. 2019; 123:229–39. <https://doi.org/10.1016/j.chaos.2019.04.010>.
- [35] Perisic A, Bauch CT. Social contact networks and disease eradication under voluntary vaccination. *PLoS Comput Biol* 2009;5:e1000280. <https://doi.org/10.1371/journal.pcbi.1000280>.
- [36] Jia D, Wang X, Song Z, Romic I, Li X, Jusup M, et al. Evolutionary dynamics drives role specialization in a community of players. *J R Soc Interface* 2020;17:20200174. <https://doi.org/10.1098/rsif.2020.0174>.
- [37] Tanimoto J. *Sociophysics approach to epidemics*. Springer Singapore; 2021. <https://doi.org/10.1007/978-981-33-6481-3>.
- [38] Bauch CT, DJD Earn. Vaccination and the theory of games. *Proceedings of the National Academy of Sciences* 2004;101:13391–4. <https://doi.org/10.1073/pnas.0403823101>.
- [39] Wang Z, Bauch CT, Bhattacharyya S, d'Onofrio A, Manfredi P, Perc M, et al. Statistical physics of vaccination. *Phys Rep* 2016;664:1–113. <https://doi.org/10.1016/j.physrep.2016.10.006>.
- [40] Fu F, Rosenbloom DI, Wang L, Nowak MA. Imitation dynamics of vaccination behaviour on social networks. *Proceedings of the Royal Society B* 2011;278:42–9. <https://doi.org/10.1098/rspb.2010.1107>.
- [41] Zhang H, Zhang J, Zhou C, Small M, Wang B. Hub nodes inhibit the outbreak of epidemic under voluntary vaccination. *New J Phys* 2010;12:023015. <https://doi.org/10.1088/1367-2630/12/2/023015>.
- [42] Zhang H-F, Wang Z. Suppressing epidemic spreading by imitating hub nodes' strategy. *IEEE TRANSACTIONS ON CIRCUITS AND SYSTEMS—II: EXPRESS BRIEFS* 2020;67:1979–83. <https://doi.org/10.1109/TCSII.2019.2938775>.
- [43] Kabir KMA, Kuga K, Tanimoto J. The impact of information spreading on epidemic vaccination game dynamics in a heterogeneous complex network- a theoretical approach. *Chaos, Solitons Fractals*. 2020;132. <https://doi.org/10.1016/j.chaos.2019.109548>.
- [44] Kabir KMA, Kuga K, Tanimoto J. Effect of information spreading to suppress the disease contagion on the epidemic vaccination game. *Chaos, Solitons Fractals*. 2019;119:180–7. <https://doi.org/10.1016/j.chaos.2018.12.023>.
- [45] Kabir KMA, Risa T, Tanimoto J. Prosocial behavior of wearing a mask during an epidemic: an evolutionary explanation. *Sci Rep* 2021;11:12621. <https://doi.org/10.1038/s41598-021-92094-2>.
- [46] Zou R, Duan X, Han Z, Lu Y, Ma K. What information sources can prevent the epidemic: local information or kin information? *Chaos, Solitons Fractals*. 2023; 168. <https://doi.org/10.1016/j.chaos.2023.113104>.
- [47] Jia D, Li T, Zhao Y, Zhang X, Wang Z. Empty nodes affect conditional cooperation under reinforcement learning. *Appl Math Comput* 2022;413. <https://doi.org/10.1016/j.amc.2021.126658>.
- [48] Miyaji K, Tanimoto J. The existence of fence-sitters relaxes the spatial prisoner's dilemma and enhances network reciprocity. *Appl Math Comput* 2021;390. <https://doi.org/10.1016/j.amc.2020.125624>.
- [49] Tatsukawa Y, Arefin MR, Utsumi S, Kuga K, Tanimoto J. Stochasticity of disease spreading derived from the microscopic simulation approach for various physical contact networks. *Appl Math Comput* 2022;431:127328. <https://doi.org/10.1016/j.amc.2022.127328>.
- [50] Kabir KMA, Tanimoto J. Cost-efficiency analysis of voluntary vaccination against n-serovar diseases using antibody-dependent enhancement: a game approach. *J Theor Biol* 2020;503:110379. <https://doi.org/10.1016/j.jtbi.2020.110379>.
- [51] Tori R, Tanimoto J. A study on prosocial behavior of wearing a mask and self-quarantining to prevent the spread of diseases underpinned by evolutionary game theory. *Chaos Solitons Fractals*. 2022;158:112030. <https://doi.org/10.1016/j.chaos.2022.112030>.
- [52] Utsumi S, Arefin MR, Tatsukawa Y, Tanimoto J. How and to what extent does the anti-social behavior of violating self-quarantine measures increase the spread of disease? *Chaos Solitons Fractals*. 2022;159:112178. <https://doi.org/10.1016/j.chaos.2022.112178>.
- [53] Utsumi S, Tatsukawa Y, Tanimoto J. Does a resource-storing mechanism favor “the wealthy do not fight”?—An approach from evolutionary game theory. *Chaos, Solitons Fractals*. 2022;160. <https://doi.org/10.1016/j.chaos.2022.112207>.
- [54] Shi B, Liu G, Qiu H, Wang Z, Ren Y, Chen D. Exploring voluntary vaccination with bounded rationality through reinforcement learning. *Physica A* 2019;515:171–82. <https://doi.org/10.1016/j.physa.2018.09.151>.
- [55] Ahsan Habib M, Tanaka M, Tanimoto J. How does conformity promote the enhancement of cooperation in the network reciprocity in spatial prisoner's dilemma games? *Chaos, Solitons Fractals*. 2020;138. <https://doi.org/10.1016/j.chaos.2020.109997>.
- [56] Wang X, Gao S, Zhu P, Wang J. Roles of different update strategies in the vaccination behavior on two-layered networks. *Phys Lett A* 2020;384. <https://doi.org/10.1016/j.physleta.2019.126224>.
- [57] Wang X, Jia D, Gao S, Xia C, Li X, Wang Z. Vaccination behavior by coupling the epidemic spreading with the human decision under the game theory. *Appl Math Comput* 2020;380. <https://doi.org/10.1016/j.amc.2020.125232>.
- [58] Wang X, Song Z, Li Z, Chang L, Wang Z. Delay-induced patterns in a reaction–diffusion system on complex networks. *New J Phys* 2021;23:073022. <https://doi.org/10.1088/1367-2630/ac0ebc>.
- [59] Bauch CT. Imitation dynamics predict vaccinating behaviour. *Proc Biol Sci*. 2005; 272:1669–75. <https://doi.org/10.1098/rspb.2005.3153>.
- [60] Wang H, Ma C, Chen H-S, Zhang H-F. Effects of asymptomatic infection and self-initiated awareness on the coupled disease-awareness dynamics in multiplex networks. *Appl Math Comput* 2021;400. <https://doi.org/10.1016/j.amc.2021.126084>.
- [61] Dehning J, Zierenberg J, Spitzner FP, Wibral M, Neto JP, Wilczek M, et al. Inferring change points in the spread of COVID-19 reveals the effectiveness of interventions. *Science* 2020;369. <https://doi.org/10.1126/science.abb9789>.
- [62] Perakis G, Singhvi D, Skali Lami O, Thayaparan L. COVID-19: a multiwave SIR-based model for learning waves. *Prod Oper Manag* 2022. <https://doi.org/10.1111/poms.13681>.
- [63] Fukuda E, Kokubo S, Tanimoto J, Wang Z, Hagishima A, Ikegaya N. Risk assessment for infectious disease and its impact on voluntary vaccination behavior in social networks. *Chaos, Solitons Fractals*. 2014;68:1–9. <https://doi.org/10.1016/j.chaos.2014.07.004>.
- [64] Bauch CT, Bhattacharyya S. Evolutionary game theory and social learning can determine how vaccine scares unfold. *PLoS Comput Biol* 2012;8:e1002452. <https://doi.org/10.1371/journal.pcbi.1002452>.
- [65] Kuga K, Tanimoto J. Which is more effective for suppressing an infectious disease: imperfect vaccination or defense against contagion? *J Stat Mech Theory Exp* 2018; 2018. <https://doi.org/10.1088/1742-5468/aaac3c>.
- [66] Iwamura Y, Tanimoto J. Realistic decision-making processes in a vaccination game. *Physica A* 2018;494:236–41. <https://doi.org/10.1016/j.physa.2017.11.148>.
- [67] Gyorgy Szabo, Csaba T. Evolutionary prisoner's dilemma game on a square lattice. *Phys Rev E* 1998;58:69–73. <https://doi.org/10.1103/PhysRevE.58.69>.
- [68] Traulsen A, Nowak MA, Pacheco JM. Stochastic dynamics of invasion and fixation. *Phys Rev E Stat Nonlin Soft Matter Phys* 2006;74:011909. <https://doi.org/10.1103/PhysRevE.74.011909>.
- [69] Annas S, Isbat Pratama M, Rifandi M, Sanusi W, Side S. Stability analysis and numerical simulation of SEIR model for pandemic COVID-19 spread in Indonesia. *Chaos Solitons Fractals* 2020;139:110072. <https://doi.org/10.1016/j.chaos.2020.110072>.
- [70] Pvd Driessche, Watmough J. Reproduction numbers and sub-threshold endemic equilibria for compartmental models of disease transmission. *Math Biosci* 2002; 180. [https://doi.org/10.1016/S0025-5564\(02\)00108-6](https://doi.org/10.1016/S0025-5564(02)00108-6).
- [71] Diekmann O, Heesterbeek JA, Roberts MG. The construction of next-generation matrices for compartmental epidemic models. *J R Soc Interface* 2010;7:873–85. <https://doi.org/10.1098/rsif.2009.0386>.
- [72] Mathieu E, Ritchie H, Ortiz-Ospina E, Roser M, Hasell J, Appel C, et al. A global database of COVID-19 vaccinations. *Nat Hum Behav* 2021;5:947–53. <https://doi.org/10.1038/s41562-021-01122-8>.
- [73] Cleveland WS. Robust locally weighted regression and smoothing scatterplots. *J Am Stat Assoc* 1979;74:829–36. <https://doi.org/10.1080/01621459.1979.10481038>.
- [74] Cleveland WS, Devlin SJ. Locally weighted regression: an approach to regression analysis by local fitting. *J Am Stat Assoc* 1988;83:596–610. <https://doi.org/10.1080/01621459.1988.10478639>.
- [75] Arroyo-Marioli F, Bullano F, Kucinskas S, Rondon-Moreno C. Tracking R of COVID-19: a new real-time estimation using the Kalman filter. *PLoS One*. 2021;16: e0244474. <https://doi.org/10.1371/journal.pone.0244474>.